URTeC: 5408

New Fracture Diagnostic Tool for Unconventionals: High-Resolution Distributed Strain Sensing via Rayleigh Frequency Shift during Production in Hydraulic Fracture Test 2

Gustavo A. Ugueto[1], Magdalena Wojtaszek[2], Somnath Mondal[1], Artur Guzik[3], Dana Jurick[3], Ge Jin[4],1. Shell Exploration & Production Company, 2 Brunei Shell Petroleum Co Sdn Bhd, 3 Neubrex, 4 Colorado School of Mines

ABSTRACT

Fiber Optic monitoring in unconventional reservoirs has proven to be an invaluable diagnostic tool for assessing both near-wellbore stimulation effectiveness and to help describe the far-field frac geometries created by hydraulic fracture stimulation. Unfortunately, gaining any detailed qualitative and quantitative understanding of the near-wellbore frac geometry or cluster/stage productivity during production via Fiber Optic (FO) has proven to be more difficult, particularly in wells producing liquids. A new FO diagnostic method, Distributed Strain Sensing based on Rayleigh Frequency Shift (DSS-RFS), first demonstrated for oil and gas applications in the Hydraulic Test Site 2 (HFTS2) provides new insights about the characteristics of near-wellbore-region (NWR) during production. DSS-RFS is different from other FO strain measurements because it relies on accurate measurement of frequency shifts of Rayleigh backscattered spectrum obtained by scanning the fiber with a coherent optical time-domain reflectometer with a range of laser frequencies using a tunable-wavelength laser system. Changes in strain are measured with an extremely high spatial resolution of 20 cm and with high signal-to-noise ratios over long distances. In HFTS2, strain changes for the entire wellbore have been measured twice during scheduled shut-in and reopening operations (February 2020 and September 2020). After removing temperature effects, consistent strain changes have been observed at the location of most perforation clusters. These are caused by near-wellbore fracture aperture changes due to pressure increases during shut-in within the near-wellbore fracture network. The strain-change patterns from the DSS-RFS during shut-in correlate very well with the location of clusters and allow for the definition of extending intervals with positive strain signals at each cluster and slightly compressing intervals with negative strain signals between the clusters and in the non-stimulated intervals. The locations of the measured positive strain peaks also show good correspondence to DAS acoustic intensity measurements acquired during the stimulation. The geometry and magnitude of the strain changes differ significantly between the two tested completion designs in the same well. During shut-in and reopening each cluster exhibit its own strain-change / pressure path. In addition, the September 2020 dataset also revealed the existence of small but measurable strain changes as consequence of pressure decline during production. These strain changes also correlate well with the presence of producing clusters, but the strain-rate signals are opposite to that obtained during shut-in and reopening operations. Although

we are still in the early stages of exploring the potential of this novel FO technique, we believe that the highly detailed information contained in the measurement of strain changes using DSS-RFS during production can significantly improve our understanding of near-wellbore hydraulic fracture characteristics and the relationships between stimulation and production from unconventional oil and gas wells.

Introduction

Unraveling the complex interplay between the wells, stimulation and subsurface in unconventional reservoirs requires an in-depth knowledge of the reservoir properties, frac geometries (both hydraulic and effective), the monitoring of well and reservoir pressures and a detail understanding of the production for selected stages and perforation clusters through time. Obtaining such information for many stages and wells is currently cost prohibitive. However, a concentrated and comprehensive data acquisition program within a dedicated test site can provide insights about the stimulation/subsurface interplay. The objective of a dedicated Integrated Fracture Diagnostics Pilot (IFDP) such as HFTS2 is to learn in few instrumented and observation wells so that the information gained can be applied to many other wells and pads with similar reservoir conditions. This approach towards de-risking unconventional development can provide critical information not available by other means. We believe this information would allow to balance the capital investment against the required economic returns that we get from production (Ugueto et al. 2018).

Traditionally rate allocation within a well with many production entries has been done via Production Logging Tools (PLT). Unfortunately, the current generation of PLT devices have proven unreliable and inadequate in determining the relatively low flow rates expected from individual perforation clusters in unconventional wells with hundreds of potential inflow entries. The need for tractoring or Coil Tubing (CT) to convey the PLT in horizontal wells and the inability to monitor logging/QC the data in real time has diminished the impact and value that production profiling and PLT logging could have in understanding unconventional reservoirs. Long horizontal sections made PLT tractoring and CT conveyance operations very costly and potentially risky. As a result, very few PLTs have been acquired in unconventional wells. In the rare occasions when production logs have been acquired, many clusters appear to be not producing with two-thirds of production being allocated to only one third of the perforation clusters (Miller et al. 2011). A new generation of modern and configurable PLT devices is now available (Donovan et al. 2019). Although these new tools can provide better quality production profiling and could provide better metering of the overall flow within the wellbore, differentiating the contribution of individual clusters may still prove difficult for PLTs.

FO technology have been identified as a possible solution to obtaining reliable production profiling in unconventional wells. Successful production profiling via Distributed Acoustics Sensing (DAS) have been reported in gas producing wells (Ugueto et al. 2018). Regrettably, many gas and most liquid producing wells do not generate strong enough DAS signals while flowing thus limiting the use of this technology for production profiling. Jin et al. 2019 documented a jointly inverted DTS transient temperature signal and DAS flow-velocity measurements to provide a production allocation profile across an entire well. Identification of producing clusters and possible production profiling using multiple short duration transient DTS and DAS signals have also been proposed by Attia et al. 2019, Lawrence et al. 2021 and Wu et al. 2021. However, all these new FO production profiling data acquisition protocols and workflows rely on collecting signals during short shut-in reopening cycles lasting only few minutes. The data from these tests may not represent the flowing condition during continuous stable flow. Therefore, there is still a need to develop new workflows and algorithms using high fidelity FO data that can be related to the production characteristics of individual perforation clusters.

DSS-RFS Explained

Distributed Strain Sensing Rayleigh Frequency Shift (DSS-RFS) uses Rayleigh backscatter in a non-engineered single mode fiber (SM) to measure strain changes along the fiber. The principle of the DSS-RFS method is described as follow (Jin et al. 2021): When an optical fiber is manufactured, random inhomogeneities of the glass density are created in the fiber core. The random density heterogeneities

manifest as a variation of refractive index along the fiber. For a certain laser frequency, the constructive and destructive interferences between the Rayleigh backscatters causes irregular but unique amplitude fluctuations in the coherent optical time-domain reflectometer along the fiber length. For each discrete fiber segment, a unique Rayleigh scattering spectrum is obtained by scanning the fiber with a coherent optical time-domain reflectometer with a range of laser frequencies using a tunable-wavelength laser system. This unique Rayleigh scattering spectrum shifts in frequency if the temperature and/or strain of the fiber section changes, which causes the spacing and optical delay to vary between the scatterers (Kishida et al. 2014). This measuring principle is conceptually illustrated in Figures 1a and 1b.

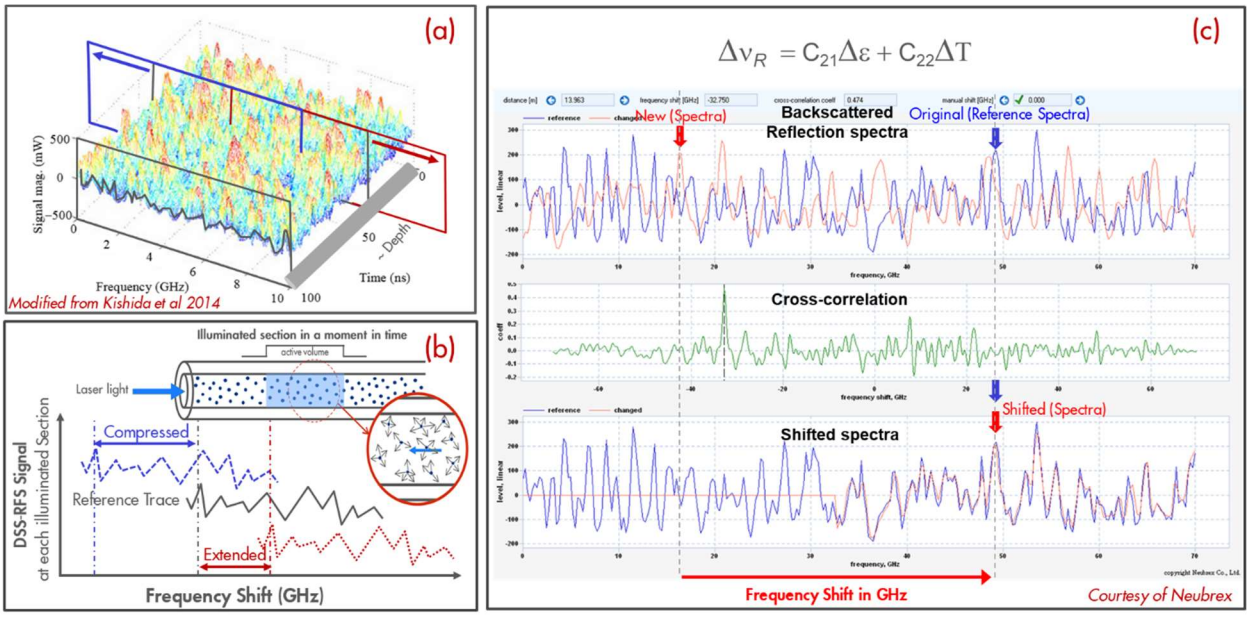

Figure 1. Illustration of Rayleigh Frequency Spectrum RFS. Conceptual response of along a fiber length (a) and for a single illuminated fiber segment (b). Example single spectra and cross-correlation workflow (c)

Figure 1c shows two reflected spectra for a given fiber segment, reference signal (blue) and new signal (red) as well as the shifted spectra after applying Neubrex frequency shift correlation algorithms. Like many other FO strain monitoring systems, DSS-RFS measures relative strain changes instead of absolute strain along the fiber. However, when compared with other DSS methods, DSS-RFS has some distinctive advantages. DSS-RFS has higher measuring sensitivity than strain measured using Brillouin optical time domain reflectometry (BOTDR), <1 με vs. > 1 με. DSS-RFS has higher spatial resolution than Low-Frequency DAS (LF-DAS), ~20 cm vs. ~3-8 m, and finally, DSS-RFS does not have the fiber sensing length restrictions of commercially available Fiber Bragg Grating (FBG) based DSS systems, 8-20km vs. ~100-500m.

The relationship between Rayleigh back-scatter spectrum frequency shift and temperature and strain change can be presented as:

$$\Delta\nu_R = C_{21}\Delta\varepsilon + C_{22}\Delta T$$

Where $\Delta\nu_R$ is the frequency shift of the Rayleigh back-scattering spectrum at a certain section of the sensing fiber, which is referred to as RFS in this paper. $\Delta\varepsilon$ and ΔT are the strain and temperature changes of the fiber section being interrogated, respectively. C_{21} and C_{22} are coefficients determined by fiber structure and materials. Although RFS can be caused by either temperature or strain variations, the temperature variations can be independently measured using Distributed Temperature Sensing (DTS) at the same time and in the same cable where RFS is being measured. If the temperature variation can be accurately measured or it is

small enough to be ignored, then the strain changes can be measured in a fully distributed manner using the RFS. Because the pattern of the Rayleigh scattering spectrum is unique for each section of sensing fiber and does not change over time, the pattern can be used to recognize the location and strain changes in sequential data acquisitions. This enables long term time-lapse strain change monitoring using the DSS-RFS without having to do continuous strain measurements (Jin et al. 2021).

DSS-RFS During Shut-in / Reopening Test Feb-2020

In February 2020, DSS-RFS data was acquired at one of the two FO instrumented wells in Hydraulic Fracture Test Site 2 (HFTS2). The RFS was measured on a single-mode fiber using a NeubrexVR SR7000 Rayleigh interrogator unit, which has a sensitivity of 0.075 GHz, equivalent to 0.5 με or 0.06 deg. C. The spatial resolution of the measurement is 20 cm, with a time sampling interval of 150 seconds. Figure 2 shows the strain-changes (Δε) after removing temperature changes from a DSS-RFS acquisition during a shut-in and reopening test performed in February 2020. The test began after establishing a baseline measurement during normal flowing conditions, then the well was shut- in for 4 days and opened again in a series of 2-hour shut-in and 1-hour producing cycles. Finally, the well was re-opened and DSS-RFS was acquired for approximately 6 hours. Figure 2a shows the strain-changes together with the measured downhole pressures. Figure 2b shows the average strain-change from day 3 across a depth range corresponding to a single stage with 10 perforation clusters (PCs). This average strain-change curve shows well defined peaks matching the position of 8 out of the 10 PCs for that stage.

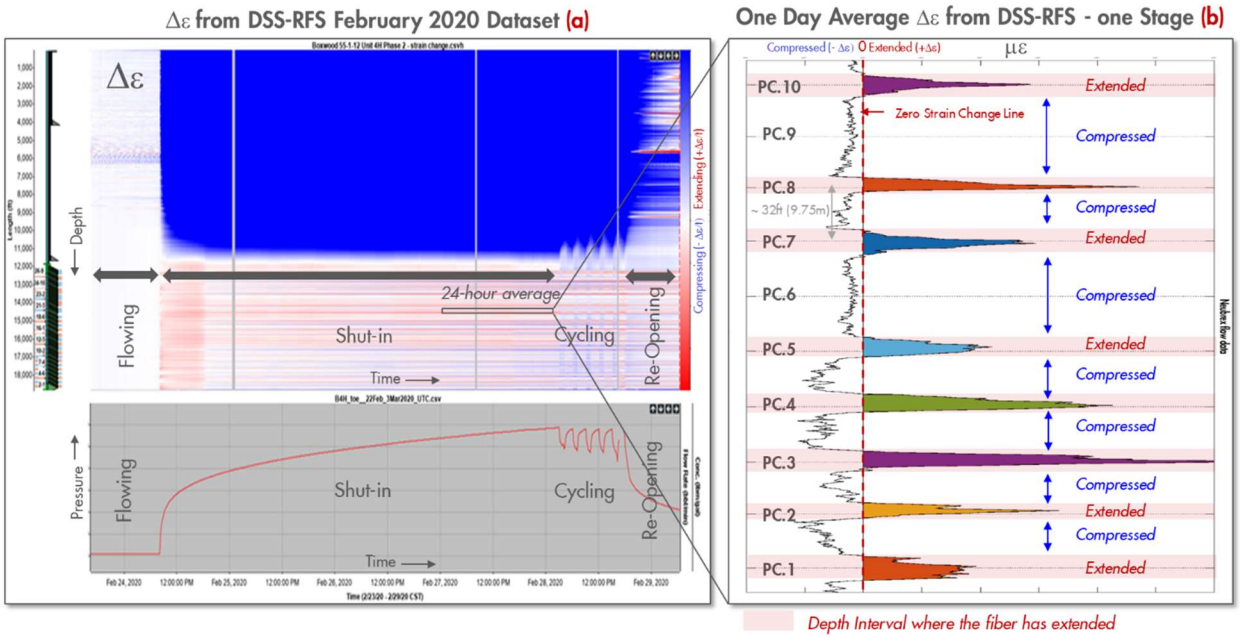

Figure 2a. Strain changes and downhole pressures acquired during shut-in and reopening during a test conducted in FO instrumented well in HFTS2. Figure 2b shows the 24-hour average strain-change response across a single stage with multiple clusters.

This DSS RFS data allows for the definition of intervals where extension has occurred corresponding to active clusters with positive strain-change signals and slightly compressed intervals with negative strain-change signals between the clusters, as well as for interval with in-active clusters.

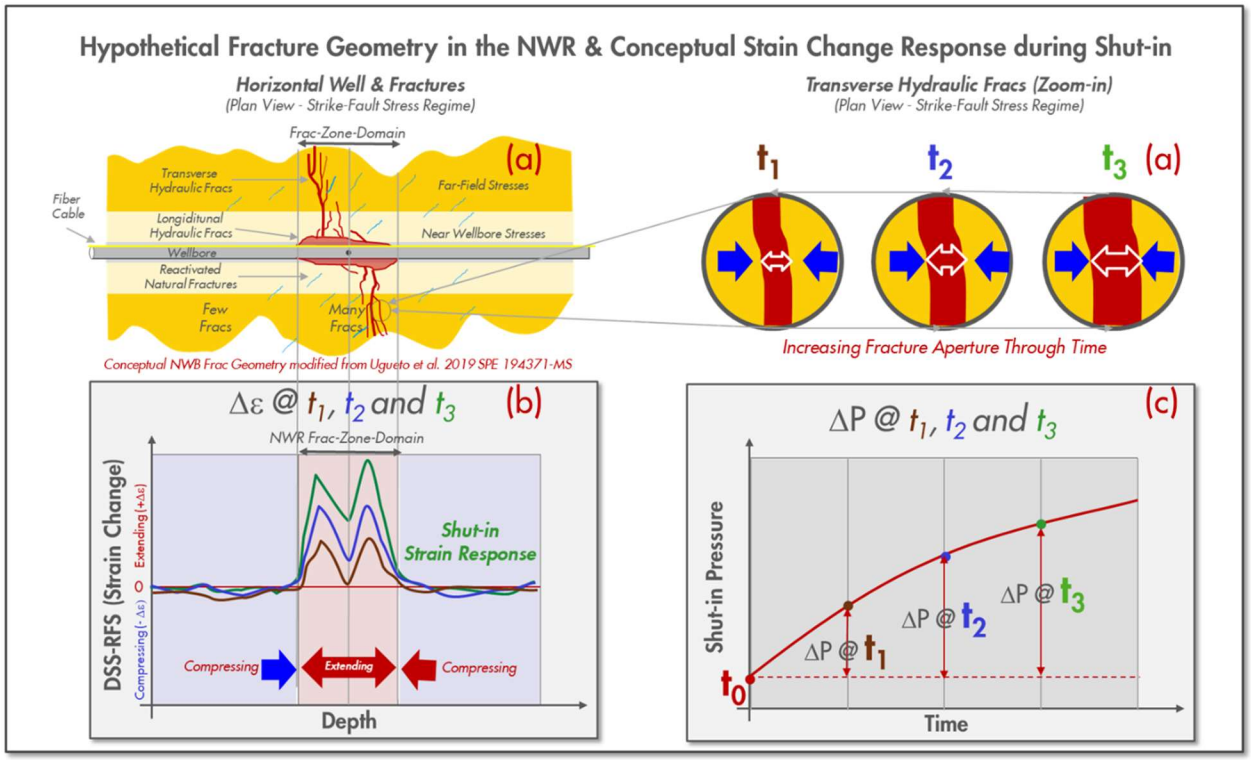

Figure 3. Hypothetical Fracture Geometry in the Near-Wellbore-Region around a single cluster (a) and conceptual strain and pressure changes during a production shut-in (b).

These signals are interpreted to be caused by fracture aperture changes due to pressure increases during shut-in within the fracture network in the NWR. Figure 3 shows a hypothetical representation of the near-wellbore environment showing a Frac-Zone-Domain consisting of hydraulic fractures generated around a single perforation cluster. The figure also shows the conceptual evolution of strain changes through time corresponding to the change in pressures within each of the fractures connected to the wellbore as result of shut-in the well. The width of the extending zone corresponds to the dimension of the frac domain created by the stimulation in the NWR. The positive strain changes after a temporary shut-in can be interpreted as fracture aperture increases caused by pressure recharging of the connected fracture network in the NWR. After the shut-in, the pressure in the fractures and the matrix pore space begin to equilibrate, decreasing the pressure drawdown between the reservoir matrix and fracture fluid, this leads to an increase in fracture aperture. This elastic mechanical response generates strain perturbations near the producing hydraulic fractures, which are detected and captured by the DSS-RFS measurements (Jin et al. 2021). Although this fracture aperture change occurs along the entire connected fracture length, the DSS-RFS measured strain changes are mostly affected by the aperture change in the fractures closer to the fiber deployed behind casing in the NWR. Figure 4 shows the average strain-change during the shut-in (day 3) in the February 2020 dataset for the entire well compared to the production period before the shut-in. Positive strain-change peaks occur across the great majority of clusters. Conversely, the space between the stages and at the heel of the well show strain changes close to zero.

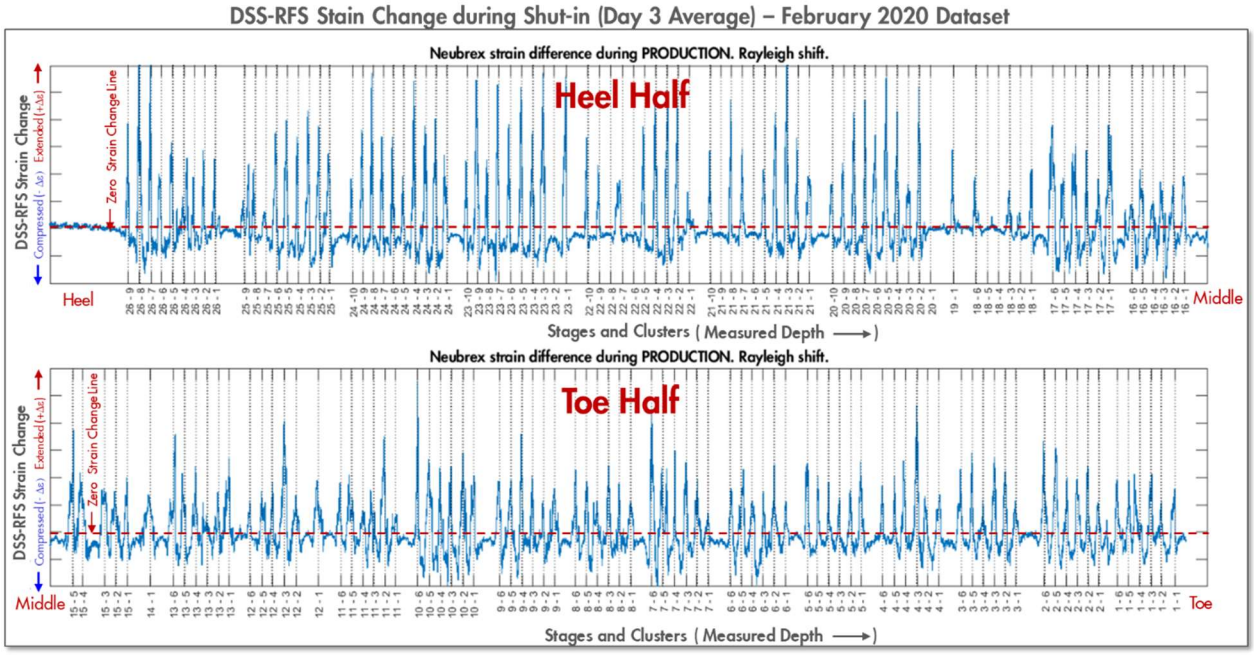

Figure 4. One day average strain-change profile across toe and heel half of FO instrumented well B4H in HFTS2-February 2020 dataset (shut-in day 3).

The acoustic intensity of the DAS signal during hydraulic fracture stimulation can serve as a good estimate of stimulation distribution efficiency and to allocate slurry to individual clusters. Figure 5 shows the comparison between the DAS acoustic intensity measurements during stimulation and DSS-RFS measurements during the February 2020 dataset for two treatment stages. In stage A, very limited DAS signal can be observed at clusters 6 and 9 during stimulation, and no positive strain changes are observed in the DSS-RFS during shut-in. The lack of DAS during stimulation and strain change peak during shut-in suggest there is no frac-zone-domain associated with these two clusters. In stage A, clusters 6 and 9 were perforated but they screened-out very early in the treatment. Stage B shows five signals in both the DAS during stimulation and DSS-RFS during shut-in. However, the spacing between the signals is different as perforation of cluster 4 was skipped due to cable mapping uncertainty around this segment of the wellbore. These two stages illustrate the high level of correspondence between placement of the frac during stimulation and the presence of active fracs during production. In this dataset the correspondence between DAS signal during stimulation and DSS-RFS during production is greater than 95%. Clusters that do not develop a positive strain change during shut-in are less likely to be the clusters that contribute to production. Hence, DSS-RFS can be used to determine the cluster efficiency during production. Figure 5 also shows that intervals with high DAS acoustic intensity signal in Stage B, at each cluster, are significantly wider than the ones in Stage A. A similar trend can be observed in the strain change measurements, with positive strain peaks in Stage B being wider and of smaller magnitudes. Because the clusters spacing are similar between these two stages, this observation supports the interpretation of Ugueto et al. 2019, who hypothesized that part of the DAS acoustic intensity signals during stimulation is also generated by the near-wellbore-region instead of the perforations only. The spatial consistency between the DAS acoustic signals during stimulation and the DSS-RFS strain changes during production indicates that DAS acoustic intensity is also controlled by the conditions in the NWR. The quality of cement between PCs, the intensity of the treatment (rate per cluster) and the rock quality all ultimately impact the characteristics of the fractures created around each cluster.

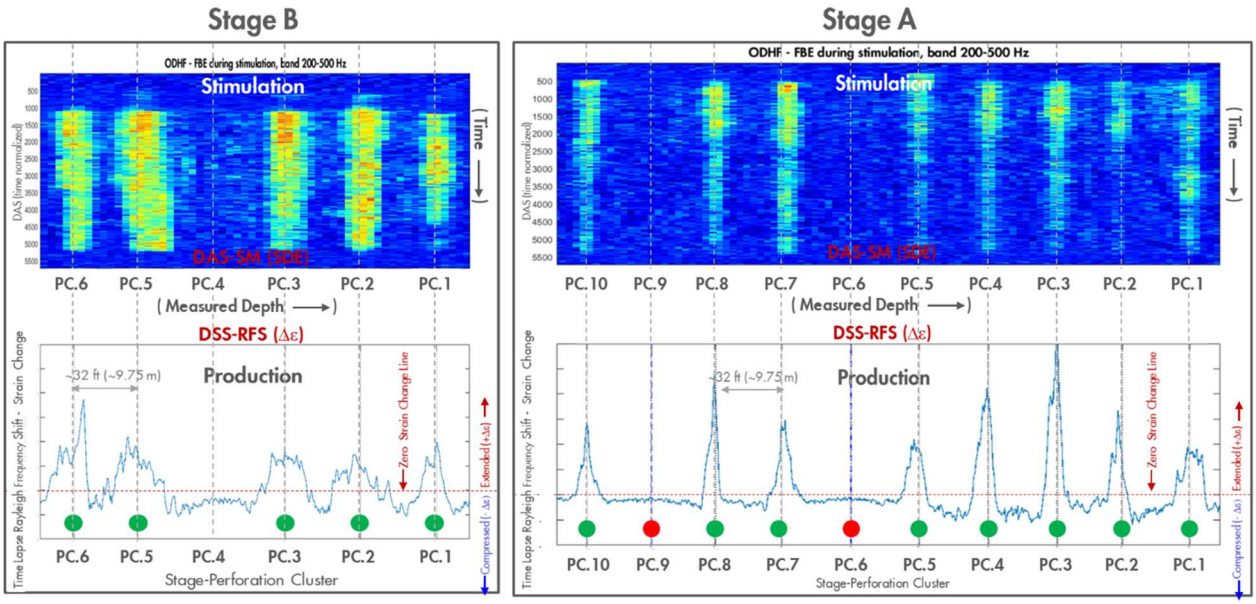

Figure 5. Comparison between DSS-RFS strain-change profiles during production shut-in and DAS acoustic intensity during stimulation for two stages. Stage A has 10 equally space perforation clusters and Stage B only has 5 clusters. Stage B was originally planned as 6 PCs stage, but PC 4 was skipped due to FO cable mapping uncertainties.

This also explains the spatial migration of DAS acoustic intensity signal near the perforation clusters during stimulation, which is commonly observed and are clearly seen at cluster 5 of Stage B. The consistency of the DSS-RFS measurements with the DAS intensity during injection also supports our interpretation that the extensional strain signals during shut-in are associated with highly conductive fracture zones in the NWR. Therefore, the shape and magnitude of the strain-change curve can be attributed to the geometry and connectivity of the fracture-zone-domain in the NWR. Several attributes can be measured from the DSS-RFS strain-change peaks. For example, the width of frac-zone-domain in the NWR can be measured. Similarly, the area of each peak can be measured by integrating the positive strain change for each perforation cluster. Figure 6 shows strong dependence of these two attributes in relation to the main two type of stimulation designs tested in this well (6 PCs Stages and 9-10 PCs Stages).

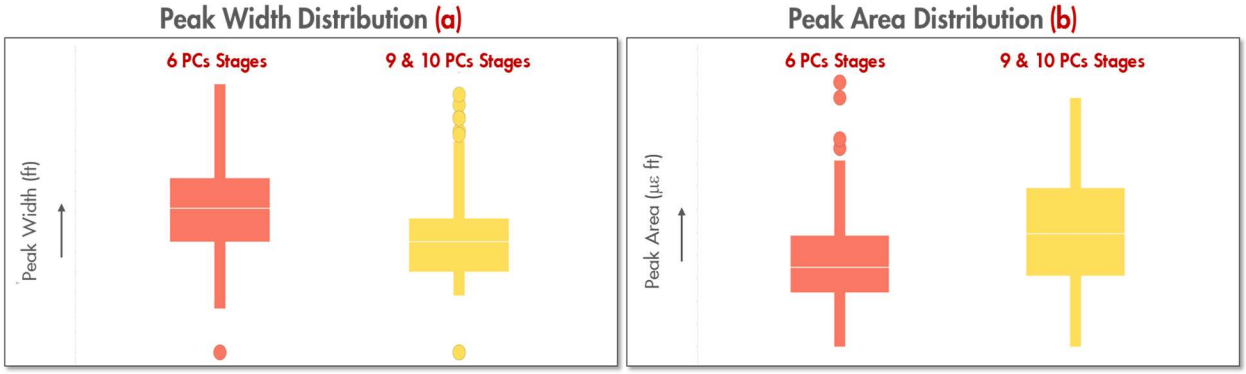

Figure 6. Example of attributes and corresponding population distribution statistics extracted from DSS-RFS strain-change profiles for the main two type of completion designs tested in HFTS2 well.

As observed in Figure 5 the peak width of 6 PCs stages are wider that those from 9 and 10 PCs stages, in average 15ft (4.6m) and 11ft (3.2m) respectively. Conversely, the peak area of the 6 PCs stages is smaller than that of 9 and 10 PCs stages. Many other attributes can be mapped from the DSS-RFS signals but these

simple statistics from relatively large samples (n=101 for 6 PCs and n=68 for 9-10 PCs stages) clearly indicate that the frac geometry and probably the production of these two designs is different.

Using DSS-RFS, strain changes can be continuously monitored at each perforation cluster during the shut-in and reopening operations. Figure 7 shows the strain changes for one perforation cluster (Fig. 7a) and for all the clusters in one stage (Fig. 7b) for the February 2020 dataset. This data indicates a strong correlation between the strain changes in the NWR as the rate of pressure increase progresses during shut-in and later decreases during reopening for each cluster. Every cluster exhibits its own "pressure strain change path". Assuming that the observed strain changes are mostly due to elastic deformation of the fractures in the NWR and resulting from the pressure changes in the wellbore, the measured strain changes can serve as proxy to the pressure changes in the near-wellbore fracture zone. However, during the shut-in period of a multi-cluster horizontal well, the interaction between the borehole and the near-wellbore fractures can be complicated due to the expected variety of conductivities between borehole and fractures in the NWR. This combined with the different recharging rates by the reservoir matrix into the fractures and possibly the occurrence of crossflow can also impact the pressure strain change path of the near-wellbore fractures.

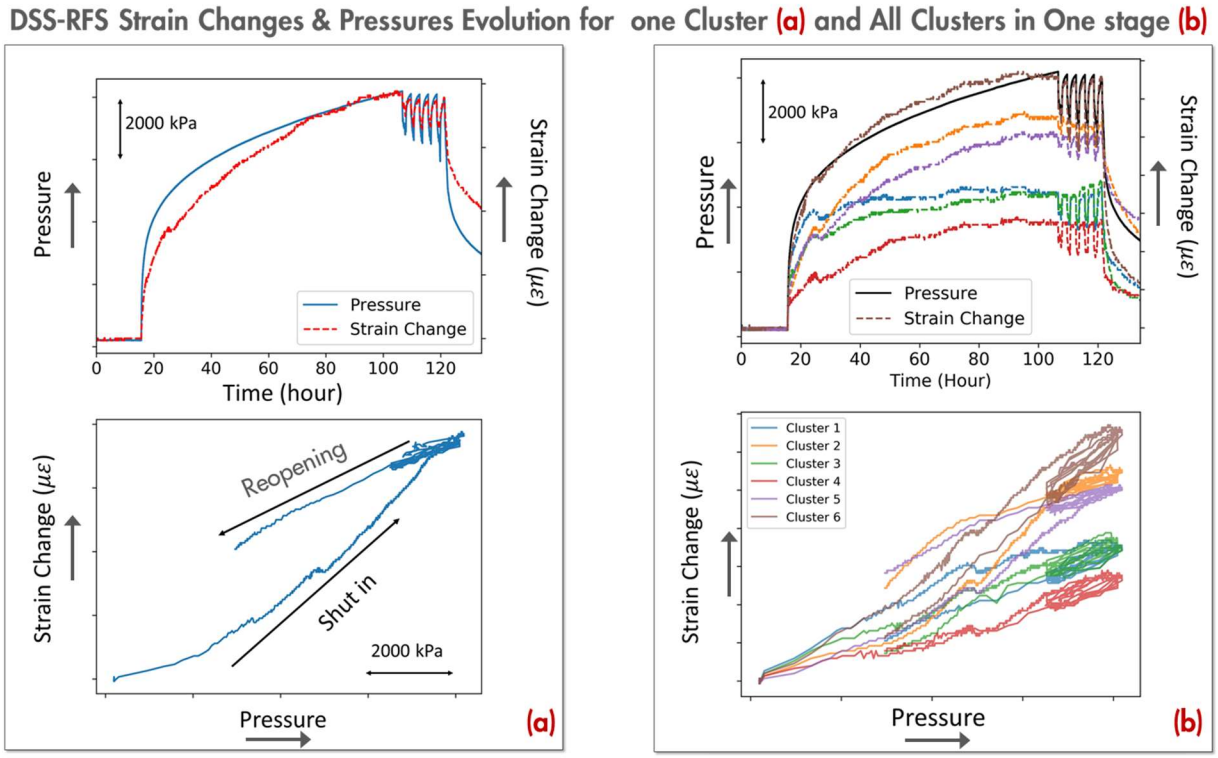

Figure 7. DSS-RFS strain-change time evolution and comparison with wellbore pressure for one cluster (a) and for all the clusters in one stage (b).

After the well is reopened, fractures with lower connectivity or higher recharging rates to the borehole may show larger discrepancies on the pressure-strain relationship curves between the shut-in and reopening paths, as illustrated in the lower panels of Figure 7a and 7b. We believe that these different "pressure strain change path" curves that include shut-in and reopening can be numerically modeled to explain and quantify the near-wellbore fracture properties and production information from this type of dataset (Liu et al. 2021).

DSS-RFS Shut-in and Reopening Test Sep-2020 and Comparison with Feb-2020 Dataset

In September 2020 a second DSS-RFS dataset was acquired in HFTS2 with the objective of determining if the new signals were like those obtained in February 2020 and to quantify any changes in the observations after 7 months of additional production. Figure 8 shows the strain changes from February 26th and

September 17th, 2020 over the entire well. This comparison was made using the DSS-RFS changes corresponding to the same amount of pressure built-up (1000 psi) for both shut-in periods. The strain changes results are very consistent, showing positive strain-change peak associated with cluster locations, no strain across non-stimulated intervals and smaller negative strain changes between the clusters.

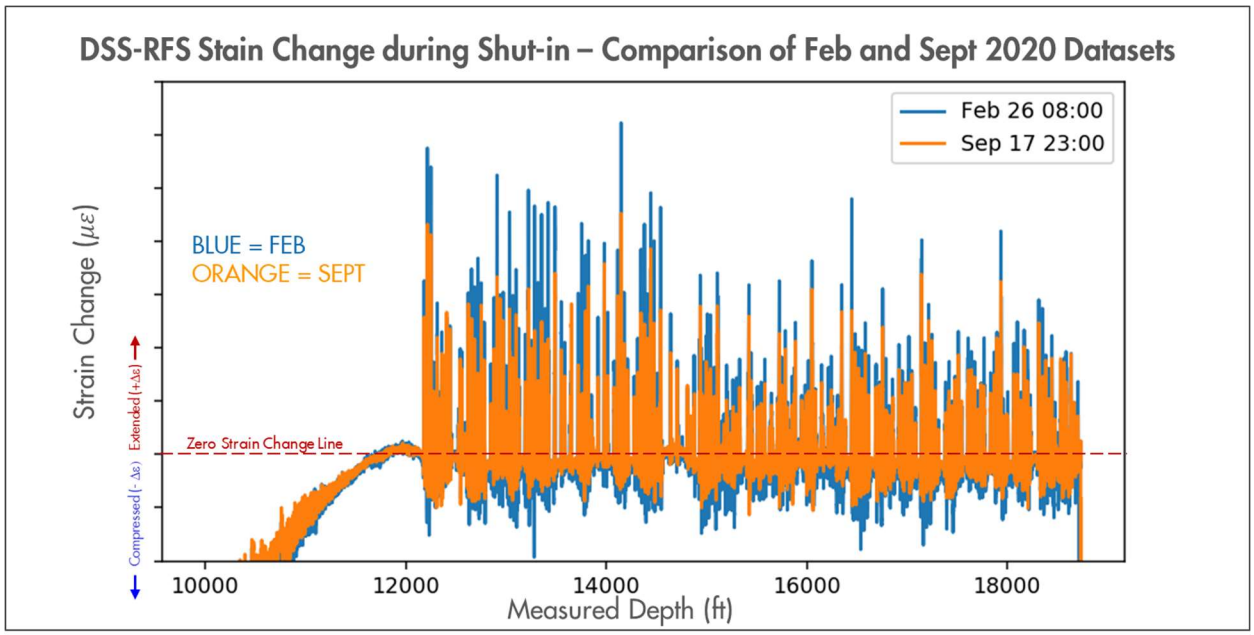

Figure 8. Comparison across the entire B4H well of the DSS-RFS strain-change profiles during shut-in on the same HFTS2 well during two separate acquisitions seven month apart, February and September 2020.

Figure 9 shows the comparison of the February and September datasets for one stage with 9 PCs. In general, the location and shape of the positive strain-change peaks are similar, but overall, the maximum strain changes are smaller in the September dataset. The strain change signals from some clusters are almost identical in PC1 and PC2, but in other cluster such as PC8 and PC9 show lesser peak width and area in the September dataset. These changes reflect the evolution of the frac-zone-domain in the NWR over the additional 7 months of production. Therefore, confirming that DSS-RFS can be used for time-lapse observations.

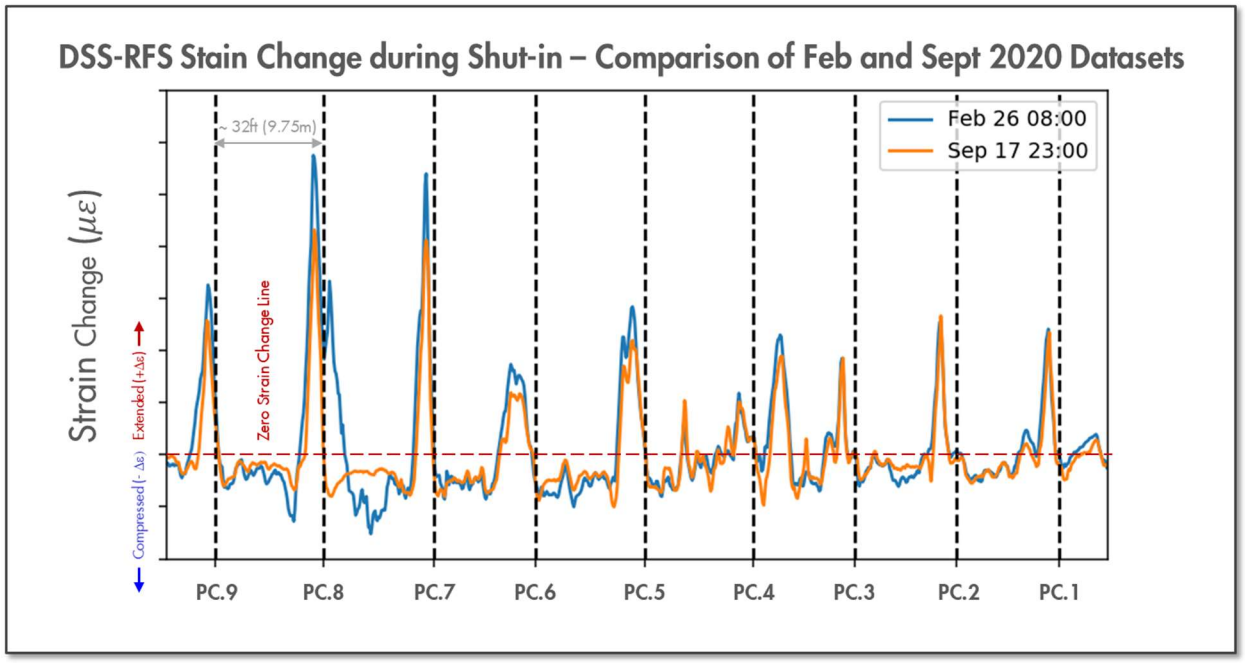

Figure 9. Comparison across one stage of the DSS-RFS strain-change profiles during shut-in for two separate acquisitions seven month apart, February and September 2020.

Figures 10 shows the comparison between two attributes from the shut-in in February and September datasets. Overall, the strain-change peaks are 24% to 32% smaller in September with the data corresponding to stages with larger number of clusters showing the bigger differences. The strain change area attribute shows a somewhat similar result but larger difference between the two datasets, indicating a reduction of 36% and 48% during the additional 7 months of production, with the bigger changes occurring on the stages with larger number of clusters. These changes can be the results of production over 7 months. We note that in this well the total liquid rate and pressure have declined by around 37% and 24% respectively over the same period, thus supporting the hypothesis that the observed strain-changes reflects the changing conditions in the well due to depletion.

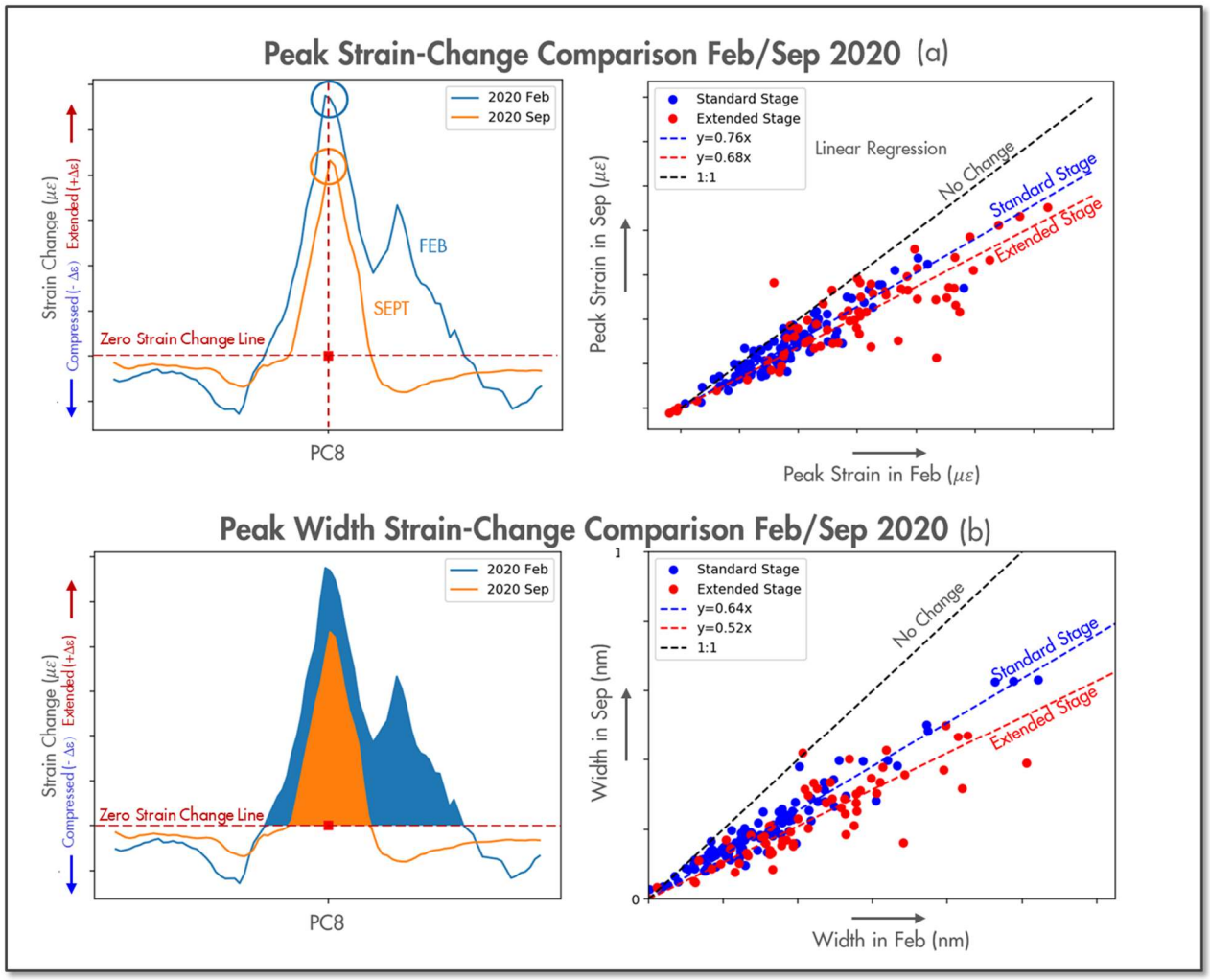

Figure 10. Changes in DSS-RFS strain-change for attributes: maximum peak and area, after 7 months of production.

The comparison of the pressure strain-change paths corresponding to individual clusters seem to indicate that most productive clusters remain the same after 7 months of production. Figure 11 shows the pressure strain-change paths for all clusters in an entire stage. Strain-change for each cluster is plotted against the pressure change (delta pressure) during the shut-in (pressure built-up) and reopening (pressure decline). In this stage, both datasets show no strain-change signals in the non-stimulated clusters (PC6 and PC7). The pressure strain-change paths for PC1 and PC9 are similar in both datasets, generally showing a low slope and similar path during shut-in and reopening. This response probably represents low producing clusters. Other PC2, 3, 4 and 5 have paths that represent productive clusters. Only two PCs (8 and 10) show paths that are different in the February and September datasets. This stage is representative of other stages in this well where characteristics of the pressure strain-change paths from February and September are similar for most of the clusters.

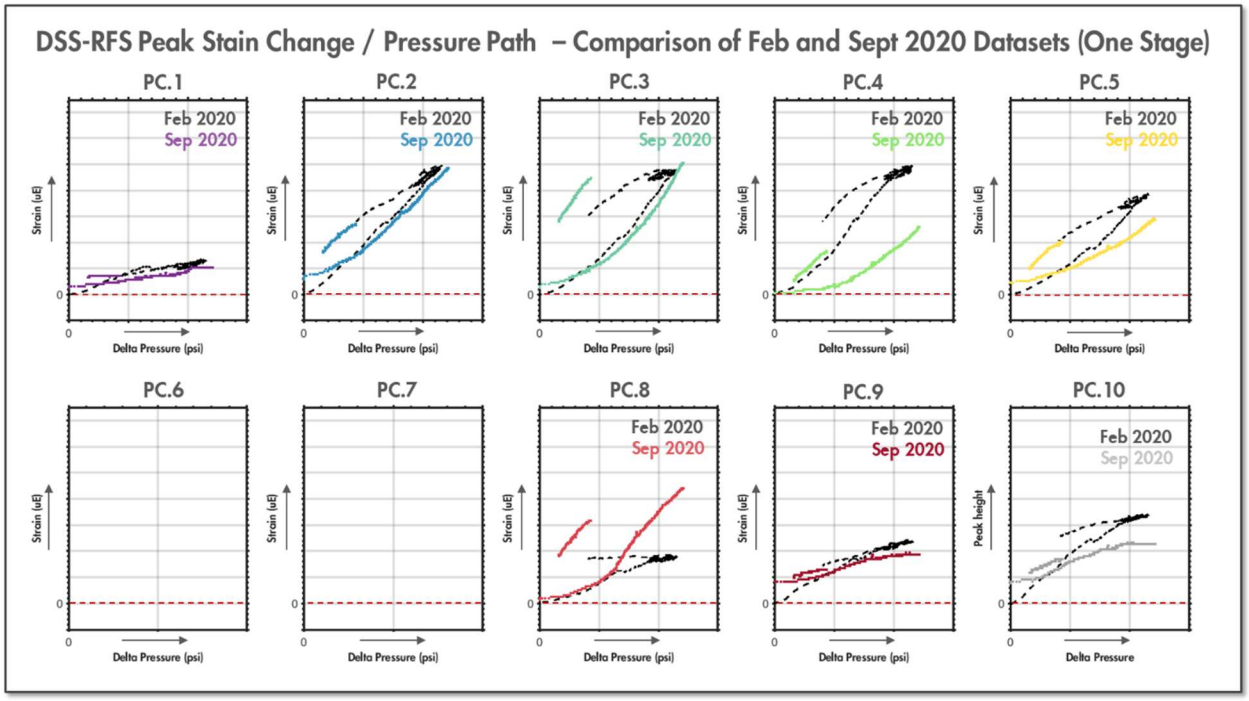

Figure 11. DSS-RFS strain-change time evolution for all clusters in one stage and comparison between the pressure strain-change path acquired in February and September 2020 datasets.

DSS-RFS during Stable Production – September 2020 Dataset

An additional objective of the September dataset was to look for the existence of any high-fidelity strain-change signals that could be obtained by monitoring DSS-RFS during stable production. We expected the signals to be small given the anticipated low rate of decline within the observation period of only one day (corresponding ~30-40 psi/day pressure decline).

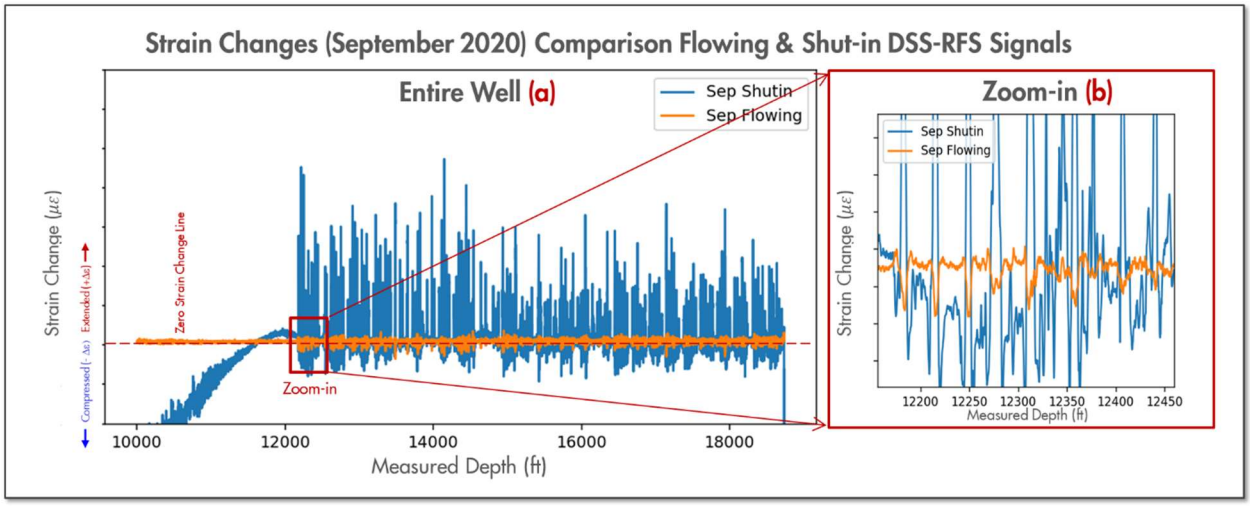

Figure 12. DSS-RFS Strain-change profile during stable flowing conditions and comparison with the strain-change profile during shut-in (September 2020 Dataset).

Figure 12a shows the one-day strain-changes while flowing (Sep 14th) and the signals acquired later during shut-in (Sep-17th) for the entire well. Figure 12b show the signals across one stage. As expected, the signals obtained while flowing are small and show strain-changes that are opposite to that acquired during shut-in, but remarkably these signals also match very well the location of active clusters. Figure 13 explains the

hypothetical strain response during stable production. Like the strain-changes recorded during shut-in we expect these signals during stable flow to be the result of the elastic deformation of the fractures in the NWR. These negative strain-change signals are the consequence of the reduction in aperture of the fractures as fluids are being drained from connected fractures and somewhat recharged by the reservoir.

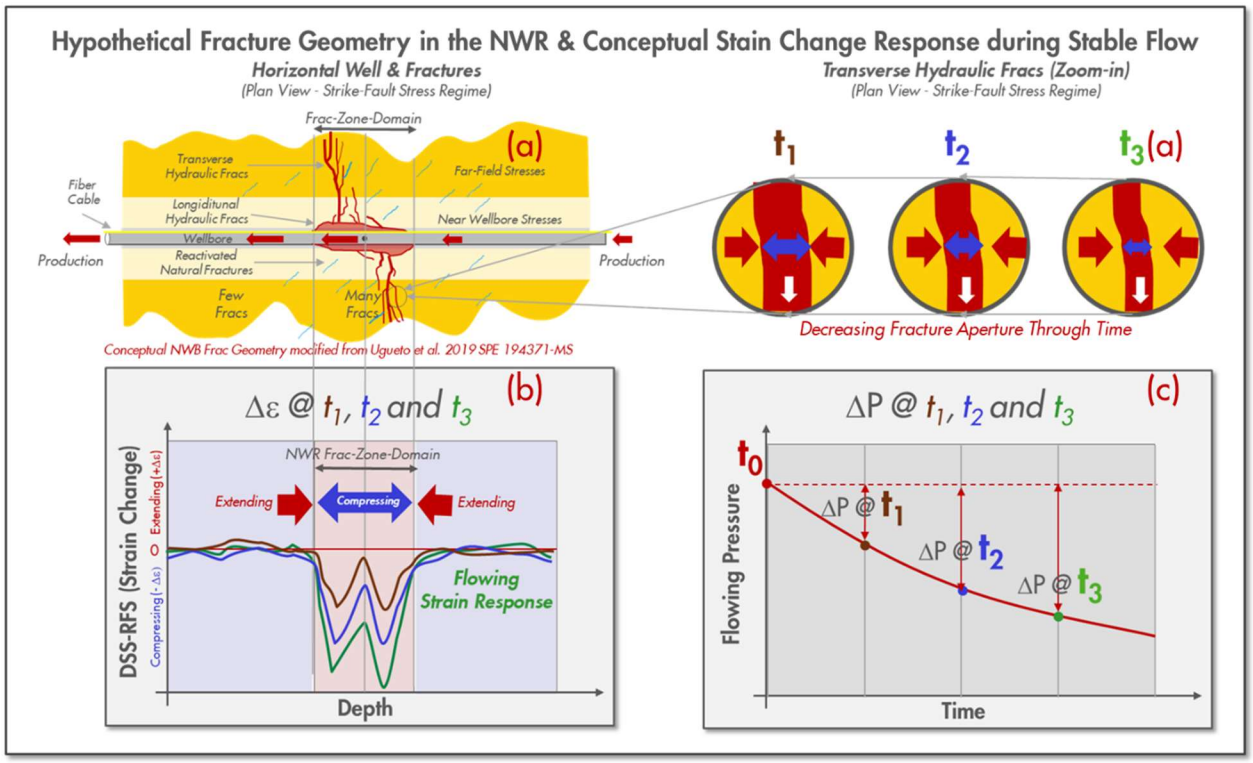

Figure 13. Hypothetical Fracture Geometry in the Near-Wellbore-Region around a single cluster (a) and conceptual strain and pressure changes during stable flow (b and c).

In order to facilitate the comparison of the shut-in strain-changes resulting from relatively large pressure perturbation during shut-in (~1000 psi) against the smaller perturbation during stable flow (~30-40 psi), the strain-changes during flow were flipped and amplified by applying a somewhat arbitrary -13.3 scaling factor. Figure 14 shows the comparison of the strain-rate signals, shut-in and flowing, for a 9 PCs and 6 PCs stages after applying the scaling factor. Although the signals obtained during stable flow are noisier, in general there is great correspondence between the characteristics of the frac-zone-domains at each cluster. However, both shut-in and flowing datasets suggest wider frac-zone-domains for the 6 PCs than for 9PCs stages. Also, the relative intensity of the peaks matches very well between flowing and shut-in acquisitions.

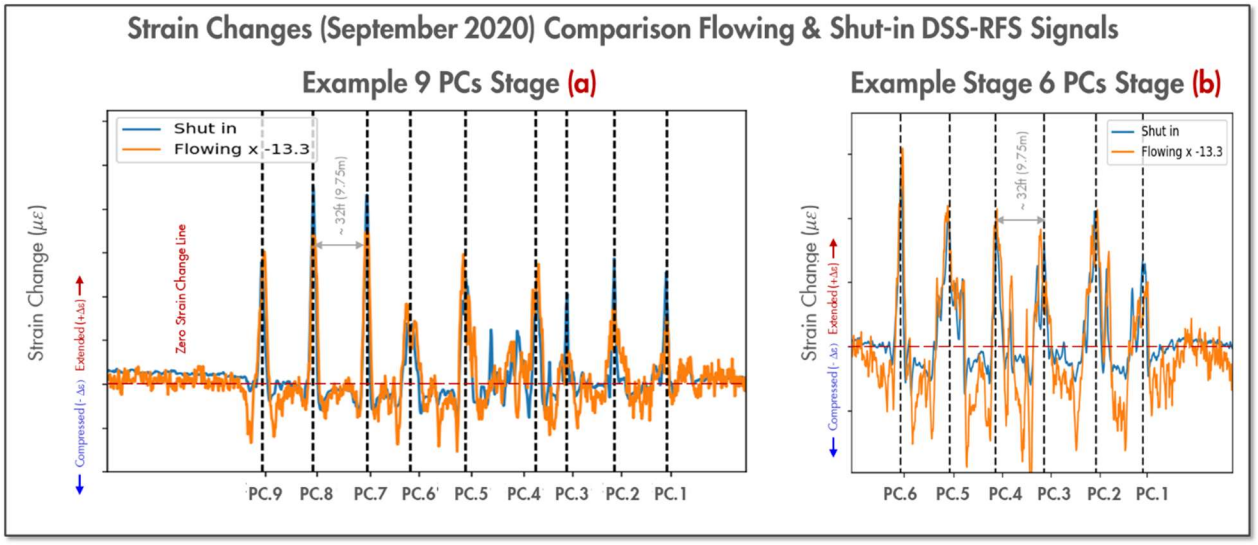

Figure 14. Comparison of DSS-RFS strain-change profiles obtained during shut-in (blue) and flipped/amplified profile acquired during stable flow (orange) for two stages with different number of clusters.

The detailed comparison of the attributes for all the clusters indicates somewhat larger, wider geometry during flowing than that observed during shut-in, suggesting a slightly larger frac-zone-domain during drainage. Figure 15 shows the geometry comparison for two clusters and corresponding statistics. Like the observations made for the shut-in datasets, the data suggest also some difference between the 9-10 PCs and 6 PCs stages.

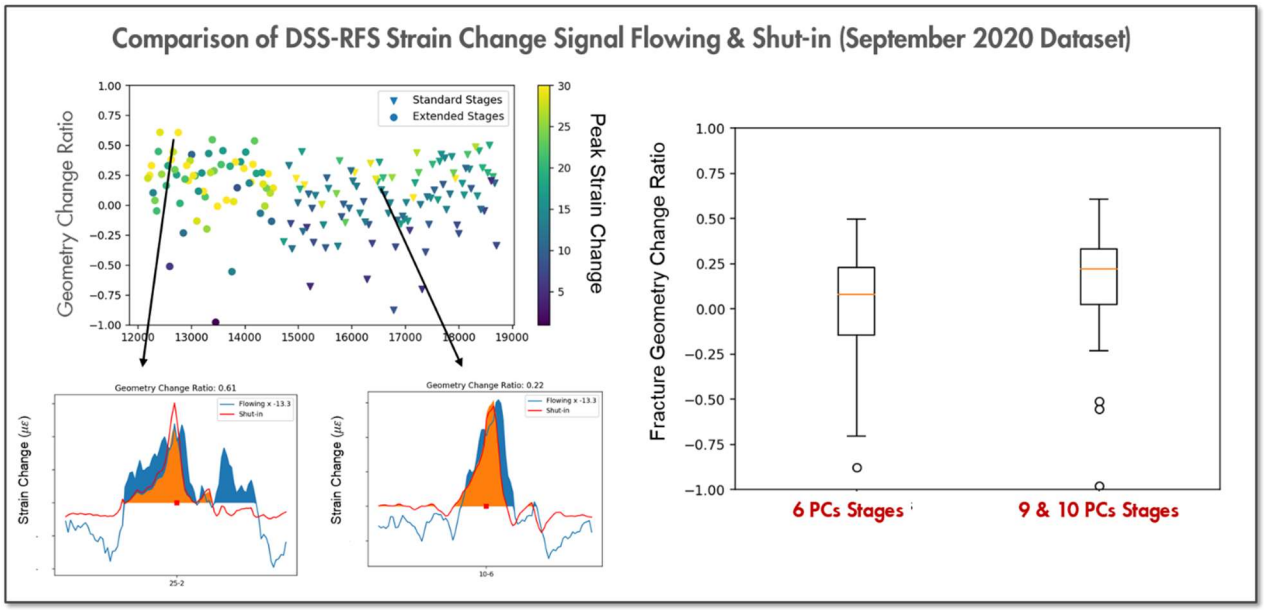

Figure 15. Comparison of DSS-RFS strain-change attributes and corresponding statistics for two types of stimulation design

As flowing pressure inside the well is similar across most clusters, we expect these signals obtained during stable flow to provide the best indication of the relative production from all the clusters. These signals can be acquired without the need to shut-in the well thus minimizing impact on well production and therefore enabling a more frequent time-lapse collection of these type of DSS-RFS signals. We anticipate that both the acquisition of the multiple flowing and shut-in/reopening datasets will provide unique information

required to better understand important aspects of the production and productivity of individual cluster never obtained before.

Conclusions

In this paper we introduce the use of DSS-RFS during production to evaluate near-wellbore fracture characteristics related to frac geometry in the NWR and cluster productivity for unconventional wells with hundreds of potential inflow entries. We believe this breakthrough application of strain monitoring provides important information related to the near borehole pressure changes at each perforation cluster.

- The strain changes obtained via DSS-RFS can be determined at high spatial resolution of 20 cm and with high temporal sampling rates.
- This high-fidelity production related data can be acquired during stable flow as well as during shut-in and reopening well operations.
- The observed strain-change variations are interpreted to be the result of near-wellbore fracture aperture changes over time and space.
- The shape and magnitude of the strain change peaks are related to the geometry of conductive near-wellbore fracture zones.
- In HFTS2 we observed near-wellbore "frac-zone-domains": with average widths ranging between 15ft (4.6m) and 11ft (3.2m).
- In HFTS2, significant differences can be observed between the two main types of stimulation and completion designs.
- The time dependent relation between borehole pressure and strain changes can provide important insights into near-wellbore fracture conductivity and reservoir recharge rate.

We anticipate that the innovation described here in using distributed fiber-optic strain sensing measurements will improve our understanding of the near-wellbore hydraulic fracture characteristics and the interaction between stimulation design and production yield in unconventional reservoirs.

Acknowledgments

First, we want to acknowledge NETL/DOE, Gas Technology Institute (GTI) and Hydraulic Fracture Test Site 2 participants for making this project possible and supporting the acquisition of these comprehensive datasets. We also thank the managements of Shell Exploration and Production Company and Neubrex Energy Services, LLC, and Neubrex Co., Ltd. for their support in the processing, analysis and interpretation of the DSS RFS data. We want to acknowledge Occidental for their support and field coordination in the acquisition of these important datasets.

Finally, we want to acknowledge individuals for their significant contribution to the HFTS2 projects particularly in the early stages of this project and during the acquisition of the DSS RFS datasets used in this paper; Alan Reynolds, Jordan Ciezobka, Scott Reeves, Gary Covatch, Kate Orsini, Vinay Sahni and Kyle Friehauf.

DOE Acknowledgment: "This material is based upon work supported by the Department of Energy under Award Number DE-FE0031577."

Reference herein to any specific commercial product, process, or service by trade name, trademark, manufacturer, or otherwise does not necessarily constitute or imply its endorsement, recommendation, or favoring by the United States Government or any agency thereof. The views and opinions of authors expressed herein do not necessarily state or reflect those of the United States Government or any agency thereof."

References

Ahmed Attia; Jared Brady; Matthew Lawrence; Robert Porter (2019). "Validating Refrac Effectiveness with Carbon Rod Conveyed Distributed Fiber Optics in the Barnett Shale for Devon Energy" D031S008R005. DOI: 10.2118/194338-MS

Glenn Donovan; Sagar Kamath; Elizabeth Tanis; Linda Abbassi; Alain Gysen (2019). "Third Generation Production Logging Technologies Enhance Inflow Profiling in Deepwater Gulf of Mexico Reservoirs". D031S048R007. DOI: 10.2118/196188-M

Jin, G., Friehauf, K., Roy, B. et al. (2019). "Fiber Optic Sensing-Based Production Logging Methods for Low-Rate Oil Producers. Paper presented at the SPE/AAPG/SEG Unconventional Resources Technology" Conference, Denver, Colorado, USA, 22–24 July. URTEC-2019-943-MS. https://doi.org/10.15530/

Jin, G., Ugueto, G., Wojtaszek, M., Guzik, A., Jurick, D. and Kishida, K., (2021). "Novel Near-Wellbore Fracture Diagnosis for Unconventional Wells Using High-Resolution Distributed Strain Sensing during Production". SPE Journal, pp.1-10.

Kishida, K., Yamauchi, Y., and Guzik, A. (2014). "Study of Optical Fibers Strain-Temperature Sensitivities Using Hybrid Brillouin-Rayleigh System". Photonic Sens 4 (1): 1–11. https://doi.org/10.1007/s13320-013-0136-1.

Liu, Y., Jin, G., Wu, K. (2021). "New Insights on Near-Wellbore Fracture Characteristics from High-Resolution Distributed Strain Sensing Measurements". Paper Presented at Unconventional Resources Technology Conference, Houston, Texas, USA, 26-28 July. URTeC-2021-5436.

Miller, C. K., Waters, G. A., & Rylander, E. I. (2011). "Evaluation of Production Log Data from Horizontal Wells Drilled in Organic Shales". Society of Petroleum Engineers. doi:10.2118/144326-MS

Matthew Lawrence and Ahmed Attia (2021). "Comparing and Combining Camera, Tracer and Distributed Temperature and Acoustic Sensing DAS+DTS for a Holistic Understanding of Stimulation and Production Performance". DOI: 10.2118/204188-MS

Ugueto C. G. A., Wojtaszek, M., Huckabee, P. T. et al. (2018). "Accelerated Stimulation Optimization via Permanent and Continuous Production Monitoring Using Fiber Optic". Paper presented at the SPE/AAPG/SEG Unconventional Resources Technology Conference, Houston, Texas, USA, 23–25 July. URTEC-2901897-MS. https://doi.org/10.15530/urtec-2018-2901897.

Ugueto, G., Huckabee, P., Wojtaszek, M. et al. (2019). "New Near-Wellbore Insights from Fiber Optics and Downhole Pressure Gauge Data". Paper presented at the SPE Hydraulic Fracturing Technology Conference and Exhibition, The Woodlands, Texas, USA, 5–7 February. SPE-194371-MS. https://doi.org/10.2118/194371-MS.